Geomechanics and Engineering, *Vol. 17, No. 5 (2019) 413-420*
DOI: https://doi.org/10.12989/gae.2019.17.5.413

Experimental study on effect of underground excavation distance on the behavior of retaining wall

Seok-Won Lee*

Department of Civil and Environmental Engineering, Konkuk University, 120 Neungdong-ro, Gwangjin-gu, Seoul 05029, Republic of Korea

(Received September 22, 2018, Revised January 17, 2019, Accepted February 5, 2019)

Abstract. The changes in earth pressure and ground settlement due to underground excavation near an existing retaining wall were studied experimentally according to the separation distance between the underground excavation and the retaining wall. In addition, this study attempted to experimentally prove that the arching phenomenon occurred during the construction of the underground space. A model tank having 120 cm in length, 160 cm in height, and 40 cm in width was manufactured to simulate underground excavation through the use of five separated base wall bodies. The variation of earth pressure on the retaining wall was measured according to the underground excavation phase through the use of 10 separated right wall bodies. The results showed that the earth pressure on the retaining wall was changed by the lowering of the first base bottom wall; however, the earth pressure was not changed significantly by the lowering of the third base bottom wall, since the third base wall had sufficient separation distance from the retaining wall. Lowering of the first base wall induced a decrease in the earth pressure in the lower part of the retaining wall; in contrast, lowering of the first base wall induced an increase in the earth pressure in the middle part of the retaining wall, proving the arching effect experimentally. It is necessary to consider the changes in earth pressure on the retaining wall in designing earth retaining structures for sections where the arching effect occurs.

Keywords: underground excavation; retaining wall; arching effect; excavation distance; model tank

1. Introduction

As a city develops, the ground space quickly becomes occupied, so underground space utilization becomes important. As the excavation of underground space becomes increasingly frequent, the existing ground structures and/or ground/underground structures in construction (e.g., earth retaining walls and tunnels) can be very close to new underground space excavation. There have been precedent studies on the individual themes, such as earth retaining walls (Altunbas *et al.* 2017, Bang 1985, Jeon *et al.* 2013, Tang and Kung 2010, Zheng *et al.* 2015) and underground excavation (Camos *et al.* 2016, Chakeri and Unver 2014, Han 2006, Mazek 2014, Son 2003, Son and Yun 2010, Yang and Li 2017, Yang and Wang 2018). An analysis of the behavior of the earth retaining wall and the changes of earth pressure by consecutive rather than individual excavations of retaining walls and underground spaces was previously carried out by Park *et al.* (2015). In addition, there have been a lot of studies on cases where the existing ground structure and the new underground excavation are close to each other (Ding *et al.* 2017, Ding *et al.* 2012, Jenck and Dias 2004, Meleki *et al.* 2011, Mroueh and Shahrour 2003, Pott and Addenbrooke 1997, Shahin *et al.* 2006, Son 2003). However, there have not been so many studies mainly focused on the behavior of the retaining wall when an underground space is excavated close to the underground retaining wall currently under construction. In other words, studies on the phenomenon in which the retaining wall of the building under construction is influenced by nearby underground excavation, are currently insufficient.

Therefore, in this study, when an underground space (e.g., tunnel) is newly built close to the area where another underground excavation has already been made by using the earth retaining wall for the construction of the ground structure, the changes of the earth pressure acting on the earth retaining wall and the surface settlement were experimentally studied. For this purpose, a large size model tank was manufactured, and sand was used as a test material. That is, a model tank with a length of 120 cm and a height of 160 cm was prepared so as to measure the earth pressure change of the earth retaining wall and the surface settlement in each underground excavation stage. The experiment was carried out in such a manner that, on the uniformly constructed sandy ground, some displacements were given to the base ground as measures such as the trap-door test and the changes in earth pressure of the vertical retaining wall and surface settlement were measured. The model test simulated underground excavation by constructing and moving 10 right wall bodies representing the earth retaining wall and five base wall bodies representing the underground excavation, in order to measure the earth pressure according to the height of the retaining wall due to the excavation of the adjacent underground space.

2. Experimental model test

2.1 Model test apparatus

For the experiment, we produced a model tank, as

*Corresponding author, Professor
E-mail: swlee@konkuk.ac.kr

http://www.techno-press.org/?journal=gae&subpage=7
ISSN: 2005-307X (Print), 2092-6219 (Online)

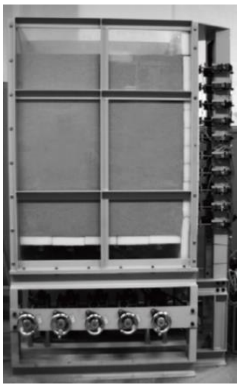

Fig. 1 Model tank with sand

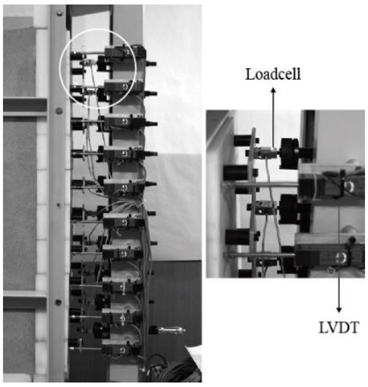

Fig. 2 LVDT installed

shown in Fig. 1. The tank had a rectangular structure with a length of 120 cm, a height of 160 cm, and a width of 40 cm. The ground was constructed by raining the sands into the tank. The size of the composed ground area was 80 cm in length, 80 cm in height, and 40 cm in width. In order to simulate the two-dimensional behavior, the material constituting the frame was made of steel having a thickness of 45 mm, so that no deformations would occur in directions other than horizontal and vertical. A 150 mm thick transparent acrylic plate was placed in front in order to observe both the ground settlement and retaining wall deformation. Steel of the same thickness was placed in the grid in order to prevent the bending of the acrylic plate.

The tank walls (right wall and base wall) were manufactured in separate parts of 10 right wall bodies and five base wall bodies in order to simulate the stepped excavations of an earth retaining wall and underground space. The size of each right wall body was 8 cm in height and 40 cm in width, and the size of each base wall body was 16 cm in length and 40 cm in width. A screw was placed on the back of each wall body so that the power could be transferred to the wall body through the rotation of the screw, allowing for either left-right or up-down movement. Since the displacement and the change of earth pressure had to be measured, load cells and LVDTs (linear variable displacement transformer) were placed, as shown in Figs. 2 and 3, in the space where the screw was placed.

Surface settlement is inevitable with the artificial movement of the retaining wall. In this experiment, the surface settlement measurement system was manufactured, as shown in Fig. 4, to measure the ground displacement.

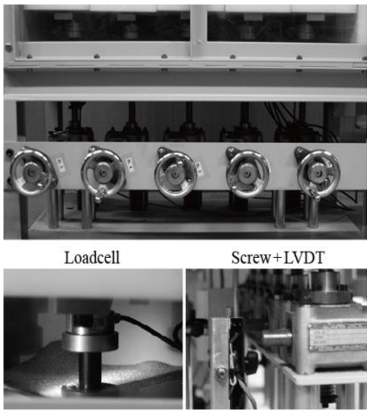

Fig. 3 Load cell installed

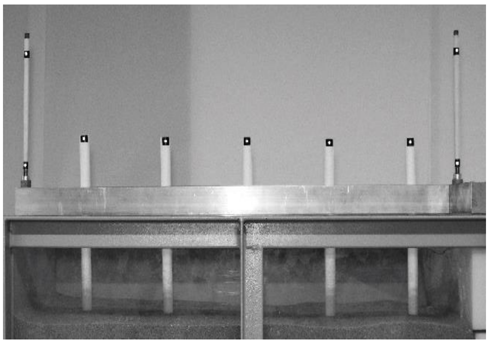

Fig. 4 Measurement of surface settlement

The rod measuring the settlement amount was made of styrofoam in order to avoid settlement due to its own weight; its diameter was 2 cm and its length 20 cm. A T-shaped bar was designed to hold the styrofoam rod, and the holes were drilled with the same diameter as the rod so as to facilitate their up-down movement; the holes were arranged at regular intervals. A camera and commercial software Photo-modeler 5 pro were used to calculate the surface settlement through photogrammetry.

2.2 Experimental test conditions and procedures

2.2.1 Test material

Jumunjin sand was used for the ground formation. Table 1 shows the physical properties of the sand used. In order to maintain and confirm the constant unit weight every time the ground was constructed, the unit weight measuring cans were buried at depths of 20 cm, 40 cm, and 60 cm, and the unit weights inside the cans were measured upon completion of the experiment. The average unit weight of the ground was 12.4 kN/m^3.

The purpose of this study is to qualitatively study the behavior of adjacent retaining walls and ground arching effect with underground excavation. Therefore, sand was used as a ground material so that the ground arching effect can be maximized experimentally. Therefore, it may be similar to the results obtained in this study qualitatively in the ground such as cohesive soil and rock mass, but the quantitative value may be different.

2.2.2 Experimental test conditions

The purpose of this test is to measure the changes in

Table 1 Physical properties of sand

Uniformity coefficient, Cu	Coefficient of gradation, Cc	Specific gravity, Gs	USCS
1.53	0.87	2.63	SP

earth pressure and surface settlement when a new excavation of underground space is made next to an existing earth retaining wall. In order to perform this experiment, the existing earth retaining wall was simulated by the right wall, as shown in Fig. 5. In order to measure the earth pressure at each height of retaining wall during the experiment, the total right wall was divided into 10 wall bodies (W1 ~ W10 in Fig. 5). Then, a total of 10 earth pressure load cells and 10 LVDTs were installed, one of each on every wall body. In order to simulate the underground space excavation adjacent to the retaining wall, the base wall was divided into five wall bodies (B1 ~ B5 in Fig. 5) and the underground excavation was activated by generating displacements in each wall body. In order to simulate the underground excavation at a certain distance from the retaining wall, one of the five base wall bodies is selected, and the base displacement is generated step by step (phases 1-7).

2.2.3 Experimental test procedures

The experiment test was conducted as follows using the above-mentioned model tank: First, the wall bodies were leveled. Then, the sand was rained into the tank 10 times by 8 cm at a time so as to form a total of 80 cm of model ground. A compaction rod of 1.0 kg was used to compact the model ground 25 times at constant intervals. After the ground composition was completed, a T-shaped bar was installed at the top of the tank, and five styrofoam rods with measuring points were placed on the tank at regular intervals.

Fig. 5 shows the modelling of phases 1 to 7 only for the base first wall body (B1 in Fig. 5). Here, each phase represents a 1 mm lowering of the base wall body. This means that if the experiment is completed up to phase 7, the wall body has been lowered down to a total of 7 mm. It can be seen that the base first wall is similar to the case where the underground space is excavated with the separation distance of 0.1H (8 cm) from the earth retaining wall. Here, H is the height of the retaining wall (80 cm). Therefore, the base second, third, fourth, and fifth wall bodies represent 0.3H, 0.5H, 0.7H, and 0.9H, respectively.

The whole experiment was carried out through this division into five cases from the base first to the base fifth walls. As described above, in order to clearly comprehend the changes of earth pressure of the retaining wall, the displacement range of the base wall was set at 0.009H (7 mm). All of the procedures of the experiment were measured with the load cells and LVDTs, and recorded in the spreadsheet using a PC and data logger.

The purpose of this study is to investigate the behavior of retaining walls and ground arching effect due to the excavation of the adjacent underground space. For this purpose, the experimental equipment was simulated using a trapdoor test device (Ahmadi and Hosseininia 2018,

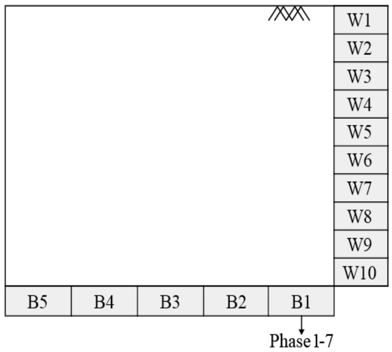

Fig. 5 Experimental test conditions

Chevalier *et al.* 2012, Costa *et al.* 2009) widely used in underground excavation simulations. In the experiments, one base wall unit was experimented from the viewpoint of one underground space. In addition, each step of downward displacement of the base wall unit was performed to simulate the excavation process of the underground space.

3. Results of experimental model test

For the experiment, the selected base wall body was lowered through seven phases in order to simulate the underground space construction having certain separation distance from the retaining wall. The five cases of experimental testing were carried out having separation distances between the base wall and the earth retaining wall of 0.1H, 0.3H, 0.5H, 0.7H, and 0.9H, respectively. Even though five experiments were carried out, the changing tendency of earth pressure acting on the earth retaining wall was described here for only the two experiments with separation distances of 0.1H (lowering of base first wall body) and 0.5H (lowering of base third wall body), since the other test results were similar to these. However, the ground settlement was described for all five of the experiments, since the ground settlement may differ from experiment to experiment.

3.1 Variation of earth pressure acting on the retaining wall

3.1.1 Variation of earth pressure due to the lowering of base first wall body

Fig. 6 shows the earth pressure acting on the right wall (simulating the retaining wall) at each depth in phase 0 (earth pressure at rest), phase 1 (1 mm lowering of base first wall body), and phase 7 (7 mm lowering of base first wall body), respectively, due to the lowering of base first wall body. It can be seen that the earth pressure on the right wall in phase 0 was similar to the theoretical triangular lateral earth pressure distribution. Across every phase of the experiment, the earth pressure on the right wall showed the largest increase at the right third wall body (W3 in Fig. 5), and the measured value was 0.8 kPa. The location where the earth pressure decreased most was at the right ninth wall body (W9 in Fig. 5), and the measured value was 1.8 kPa.

Comparing the changes of earth pressure between phase

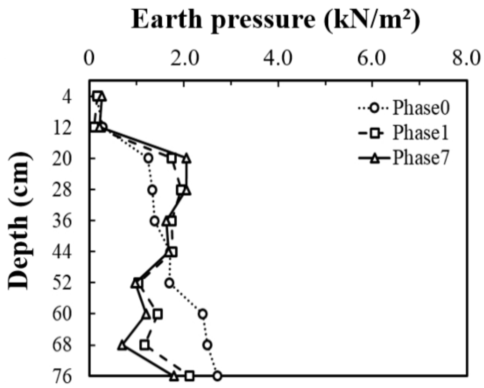

Fig. 6 Pressure variation due to B1, phases 0-7

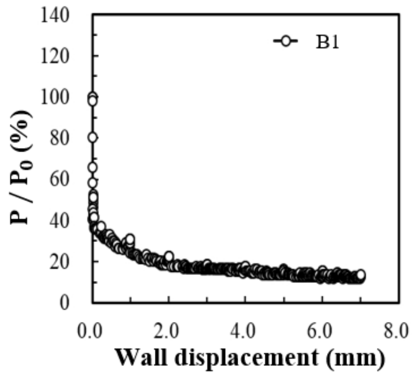

Fig. 7 Pressure on B1

0 and phase 1, it can be seen that the earth pressure on the right sixth to tenth wall bodies decreased with the movement of the base first wall body and that the earth pressure on the right third to fifth wall bodies increased. The movement of the base first wall body created an arching phenomenon such that the pressure was reduced around the right sixth to 10th walls and redistributed around the right third to fifth walls. The variation of the earth pressure around the right first to second wall bodies was relatively small, which indicates that they are beyond the range of the arching effect. Therefore, it is necessary to consider the changing earth pressure in designing an earth retaining wall for sections where the arching effect is manifested.

Comparing the earth pressure changes between phase 1 and phase 7, the earth pressure on the right seventh to 10th wall bodies decreased, and that on the right third to fourth wall bodies increased. As the movement of the base first wall body continued, the trend became the same as before, but it was smaller than the variation between phase 0 and phase 1. Thus, it can be considered that, in the dry sand condition, most earth pressure change occurred at the initial deformation.

Fig. 7 shows the changes in the earth pressure acting on the base first wall body at the movement of the base first wall body. Here, the P_0 and P refer to the initial pressure and pressure at each wall displacement, respectively. The lowering of the base first wall body caused the drop of earth pressure on the base first wall by 86.2% when compared to the initial earth pressure. Fig. 8 shows the changes in earth pressure acting on the base second and third wall bodies

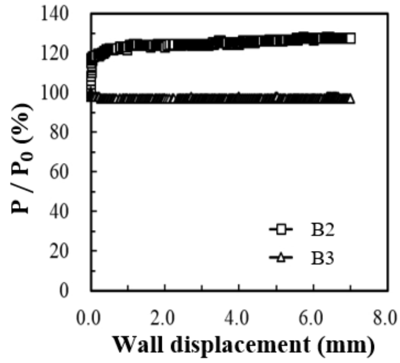

Fig. 8 Pressures on B2 and B3

(B2 and B3 in Fig. 5) at the movement of the base first wall body. The lowering of the base first wall body caused an increase of earth pressure on the base second wall by 27% compared to the initial pressure, indicating an arching effect, and the drop of earth pressure on the base third wall by just 2% compared to the initial one. Thus, it can be considered that the movement of the base first wall does not affect the earth pressure acting on the base third wall.

3.1.2 Variation of earth pressure due to the movement of base third wall body

Fig. 9 shows the earth pressure at each depth acting on the right wall (representing the retaining wall) in phase 0, phase 1, and phase 7, respectively, due to the lowering of the base third wall body. Across every phase of the experiment, the deviation of the measured earth pressure on the right walls was just -0.2~0.3 kPa. Therefore, as shown in Fig. 9, despite the change from phase 0 to phase 7

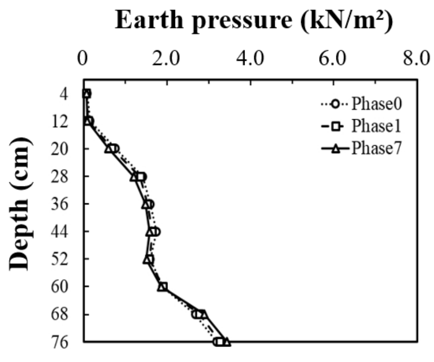

Fig. 9 Pressure variation due to B3, phases 0-7

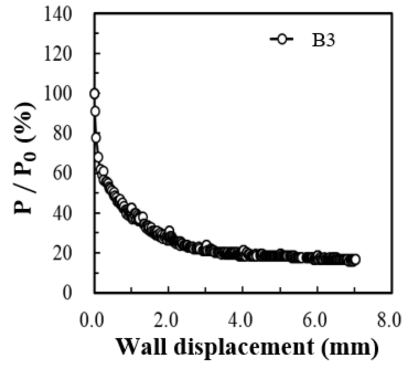

Fig. 10 Pressure on B3

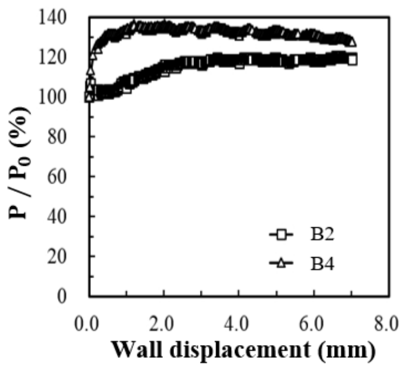

Fig. 11 Pressures on B2 and B4

(underground excavation), the earth pressure on the retaining wall changed very little. It can be considered that the movement of the base third wall (underground space excavation) did not affect the right walls (earth retaining wall), because the separation distance of the base third wall was sufficiently large at 0.5H (0.5 X height of retaining wall).

3.2 Variation of ground settlement

During the experimental test simulating the underground excavation near the retaining wall, the ground settlement was measured at each phase with photos, then analyzed using a software program. Fig. 12 shows the ground settlement up to phase 7 due to the movement of the base first wall body (0.1XH separation distance between the retaining wall and the excavation of the underground space). Fig. 13 is that due to the base second wall body (0.3XH separation distance), Fig. 14 due to the base third wall body (0.5XH separation distance), Fig. 15 due to the base fourth wall body (0.7XH separation distance), and Fig. 16 due to the base fifth wall body (0.9XH separation distance), respectively. The X axis was normalized by dividing the distance from the right wall (retaining wall) by the total length of the retaining wall (80 cm), and the Y axis was normalized by dividing the surface settlement at each phase by the maximum settlement that occurred. Table 2 shows the maximum settlement and its location according to each experimental test case. The average maximum settlement was 3.37 mm. The maximum settlement was found near the ground where the base wall body was lowered in each experiment.

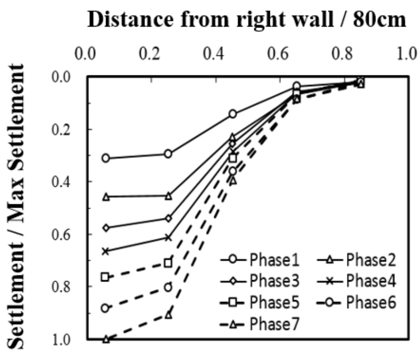

Fig. 12 Settlement due to 0.1H (B1)

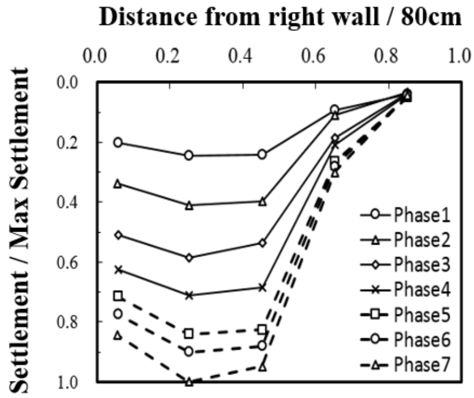

Fig. 13 Settlement due to 0.3H (B2)

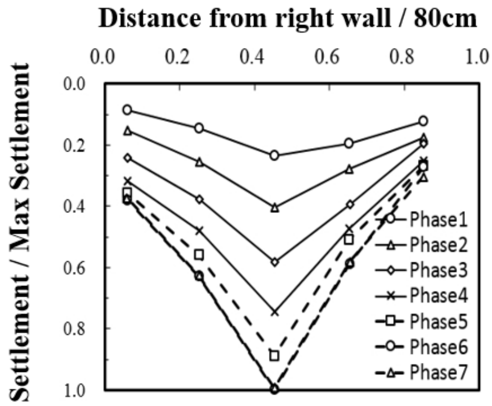

Fig. 14 Settlement due to 0.5H (B3)

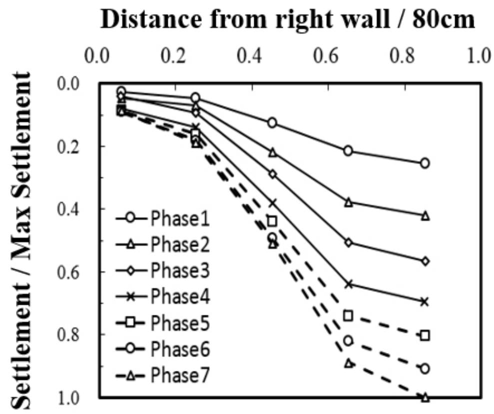

Fig. 15 Settlement due to 0.7H (B4)

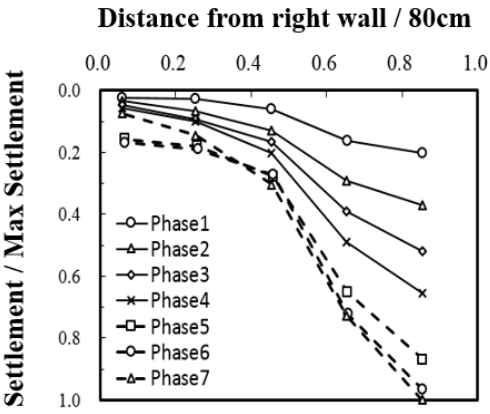

Fig. 16 Settlement due to 0.9H (B5)

Table 2 Maximum settlement and its location

Experimental test case	Maximum settlement, mm	Location of maximum settlement
B1 (0.1H, Fig. 12)	3.67	0.1H
B2 (0.3H, Fig. 13)	2.70	0.3H
B3 (0.5H, Fig. 14)	3.14	0.5H
B4 (0.7H, Fig. 15)	3.08	0.9H
B5 (0.9H, Fig. 16)	4.28	0.9H

4. Analysis of model test results

4.1 Comparison of earth pressure at the center of the retaining wall according to construction phases

Fig. 17 shows the earth pressure on the right fourth, fifth, and sixth walls (W4, W5, and W6 in Fig. 5), respectively, in each construction phase, which indicates how the lowering of the base first wall body (B1) influenced other walls during the entire experimental procedure (phases 1~7). When the base first wall body was moved, the earth pressure of the right central part (right fourth, fifth, and sixth walls) increased somewhat. Fig. 18 shows the earth pressure on the right fourth, fifth, and sixth walls (W4, W5, and W6 in Fig. 5), respectively, which indicates how the movement of the base third wall body (B3) influenced other walls during the entire experimental procedure (phases 1~7). When the base third wall body was lowered, the earth pressure of the right central part (right fourth, fifth, and sixth walls) decreased slightly, but it remained nearly constant.

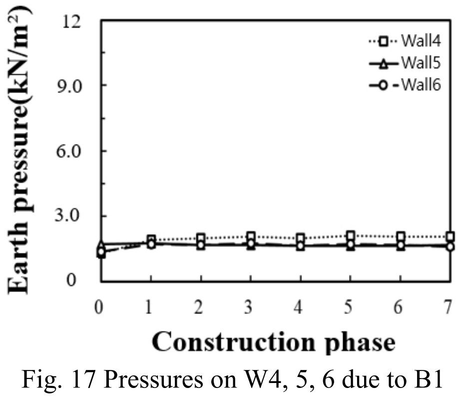

Fig. 17 Pressures on W4, 5, 6 due to B1

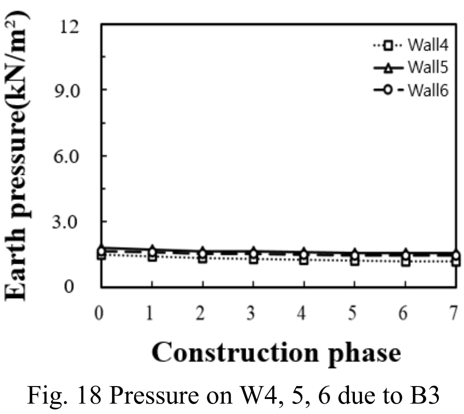

Fig. 18 Pressure on W4, 5, 6 due to B3

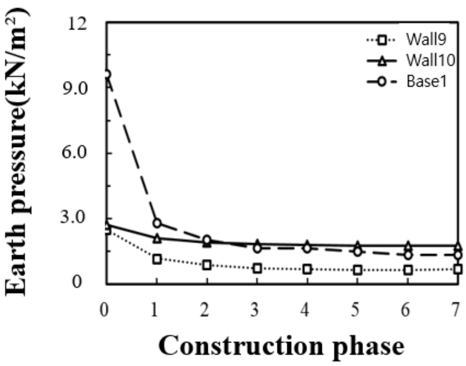

Fig. 19 Pressures on W9, 10, B1 due to B1

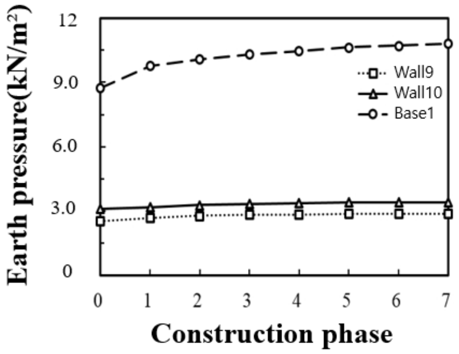

Fig. 20 Pressure on W9, 10, B1 due to B3

4.2 Comparison of earth pressure at junction of the retaining wall and underground space according to construction phases

Fig. 19 shows the earth pressure on the right ninth, 10th, and base first walls (W9, W10, and B1 in Fig. 5), respectively, in each construction phase, which indicates how the lowering of the base first wall body (B1 in Fig. 5) influenced other walls during the entire experimental procedure (phases 1~7). When the base first wall body was moved, the earth pressure on the right walls decreased. As a result of the base wall movement, it was confirmed that the ground got loose with a certain area, and the earth pressure also decreased on the right ninth and 10th walls belonging to the zone. Fig. 20 shows the earth pressure on the right ninth, 10th, and base first walls (W9, W10, and B1 in Fig. 5), respectively, in each construction phase, which indicates how the movement of the base third wall body (B3 in Fig. 5) influenced other walls in the entire experimental procedure (phases 1~7). When the base third wall body was moved, the earth pressure on the base first wall increased slightly. It can be considered that the decrease of the earth pressure on the base third wall caused that on the base first wall to increase slightly, but the earth pressures on the right ninth and 10th walls remained nearly constant.

This study has limitations in obtaining the results of the experiment using the sand in the 1g condition where the in-situ soil stress condition can not be reproduced.

5. Conclusions

In this study, experimental model tests were carried out in order to investigate the variation of earth pressure acting on the earth retaining wall due to the underground excavation nearby, according to the separation distance from the underground excavation. In addition, the ground surface settlement was measured in the case of a new underground space being built near the earth retaining wall. This study also aimed to experimentally prove that the arching phenomenon occurred during the construction of underground space. The conclusions drawn from this study are as follows:

• At the underground excavation of the base first wall body (0.1XH separation distance), the earth pressures on the right sixth to 10th walls (the lower end of the earth retaining wall) decreased, but those on the right third to fifth walls (middle of the earth retaining wall) increased. The variation of the earth pressure on the right first to second walls (upper part of the retaining wall) was relatively small. The arching phenomenon that the earth pressure around the right sixth to 10th walls was reduced, and that around the right third to fifth walls was increased due to the underground excavation of the base first wall, was proven experimentally.

• At the underground excavation of the base third wall body (0.5XH separation distance), the earth pressure on the earth retaining wall hardly changed, even when the underground excavation was simulated up to 7 mm. It can be considered that the behavior of the base third wall (underground excavation) did not affect the right wall (earth retaining wall), because the separation distance of the base third wall was sufficiently large as 0.5H (0.5Xheight of the earth retaining wall) away from the earth retaining wall.

• As a result of observing the earth pressure changes at the nearby base second and fourth walls during the excavation of the base third wall, the pressure on the base third wall became 83.2% lower than the initial pressure. However, the earth pressures on the base second and fourth walls became 18.7% and 27.5% larger than the initial pressure, respectively. This is due to the arching phenomenon, by which the pressure drop of the base third wall was redistributed to the neighboring ground.

• The measurements of ground settlement confirmed experimentally that the maximum surface settlement occurred near the ground where the excavation occurred.

• It is necessary to consider the changes in earth pressure on the retaining wall in designing an earth retaining structure for the sections where the arching effect occurs.

Acknowledgements

This research was supported by a grant (19SCIP-B105148-05) from the Construction Technology Research Program, funded by the Ministry of Land, Infrastructure, and Transport of the Korean government.

References

Ahmadi, A. and Hosseininia, E.S. (2018), "An experimental investigation on stable arch formation in cohesionless granular materials using developed trapdoor test", *Powder Technol*., **330**(1), 137-146.

Altunbas, A., Soltanbeigi, B. and Cinicioglu, O. (2017), "Determination of active failure surface geometry for cohesionless backfills", *Geomech. Eng*., **12**(6), 983-1001.

Bang, S. (1985), "Active earth pressure behind retaining walls", *J. Geotech. Eng*., **111**(3), 407-412.

Camós, C., Špačková, O., Straub, D. and Molins, C. (2016), "Probabilistic approach to assessing and monitoring settlements caused by tunneling", *Tunn. Undergr. Sp. Technol*., **51**, 313-325.

Chakeri, H. and Ünver, B. (2014), "A new equation for estimating the maximum surface settlement above tunnels excavated in soft ground", *Environ. Earth Sci*., **71**(7), 3195-3210.

Chevalier, B., Combe, G. and Villard, P. (2012), "Experimental and discrete element modeling studies of the trapdoor problem: Influence of the macro-mechanical frictional parameters", *Acta Geotech*., **7**(1), 15-39.

Costa, Y.D., Zornberg, J.G., Bueno, B. and Costa, C.L. (2009), "Failure mechanisms in sand over a deep active trapdoor", *J. Geotech. Geoenviron*., **135**(11), 1741-1753.

Ding, Z., Wei, X.J. and Wei, G. (2017), "Prediction methods on tunnel-excavation induced surface settlement around adjacent building", *Geomech. Eng*., **12**(2), 185-195

Ding, Z., Wei, X.J., Zhang, T. and Ge, G.B. (2012), "Analysis and discussion on surface settlement induced by shield tunnel construction of adjacent structure", *Disaster Adv*., **5**(4), 1656-1660.

Han, X. (2006), "The analysis and prediction of tunnelling-induced building deformation", Xi'an University of Technology, Xi'an, Shanxi, China.

Jenck, O. and Dias, D. (2004), "3D-finite difference analysis of the interaction between concrete building and shallow tunnelling", *Geotechnique*, **54**(8), 519-528.

Jeon, J.H., Park, J.D., Lim, Y.D. and Lee, S.W. (2013), "Damage assessment of structures according to the excavation methods", *J. Kor. Tunn. Undergr. Sp. Assoc*., **15**(2), 161-173.

Maleki, M., Sereshteh, H., Mousivand, M. and Bayat, M. (2011), "An equivalent beam model for the analysis of tunnel-building interaction", *Tunn. Undergr. Sp. Technol*., **26**(2), 524-533.

Mazek, S.A. (2014), "Evaluation of surface displacement equation due to tunnelling in cohesionless soil", *Geomech. Eng*., **7**(1), 55-73.

Mroueh, H. and Shahrour, I. (2003), "A full 3-D finite element analysis of tunnelling-adjacent structures interaction", *Comput. Geotech*., **30**(3), 245-253.

Park, J.D., Yu, J.S., Kim, D.Y. and Lee, S.W. (2015), "Experimental study on the ground movement due to consecutive construction of retaining wall and underground space in cohesionless soil", *J. Kor. Tunn. Undergr. Sp. Assoc*., **17**(3), 267-281.

Potts, D.M. and Addenbrooke, T.I. (1997), "A structure's influence on tunnelling-induced ground movements", *Geotech. Eng*., **110**(2), 109-125.

Shahin, H.M., Sung, E., Nakai, T. and Hinokio, M. (2006), "2D model tests and numerical simulation in shallow tunnelling considering existing building load", *Undergr. Construct. Ground Move*., **15**, 67-82.

Son, M.R. and Yun, J.C. (2010), "Comparison of ground movements in a single ground layer and multiple ground layers due to nearby tunnel excavation", *J. KSCE*, **30**(3C), 167-174.

Son, M.R. (2003), "The response of buildings to excavation-induced ground movement", Ph.D Dissertation, University of Illinois at Urbana-Champaign, Champaign, Illinois, U.S.A.

Tang, Y.G. and Kung, G.T.C. (2010), "Investigating the effect of soil models on deformations caused by braced excavations through an inverse-analysis technique", *Comput. Geotech*., **37**(6), 769-780.

Yang, X.L. and Li, W.T. (2017), "Reliability analysis of shallow tunnel with surface settlement", *Geomech. Eng*., **12**(2), 313-326.

Yang, X.L. and Wang, H.Y. (2018), “Catastrophe analysis of active-passive mechanisms for shallow tunnels with settlement”, *Geomech*. *Eng*., **15**(1), 621-630.
Zheng, D.F., Nian, T.K., Liu, B. Yin, P. and Song, L. (2015), “Coefficient charts for active earth pressures under combined loadings”, *Geomech*. *Eng*., **8**(3), 461-476.

CC